

# Breathing Training with Assistance of Laser 3D Measuring System

Klemen POVŠIČ<sup>1</sup>, Matjaž FLEŽAR<sup>2</sup>, Janez MOŽINA<sup>1</sup>, Matija JEZERŠEK<sup>1\*</sup>  
<sup>1</sup>University of Ljubljana, Faculty of Mechanical Engineering, Ljubljana, Slovenia;  
<sup>2</sup>University Clinic Golnik, Golnik, Slovenia

## Abstract

This paper presents a method for three-dimensional body shape monitoring during breathing in real-time. It is based on the laser multiple-line triangulation principle, where the laser projector illuminates the measured surface with 33 equally spaced light planes. The distorted light pattern is recorded with a camera positioned at an angle towards the measured surface. The surface displacements are displayed with a color palette, which enables the patient to correct respiratory irregularities during the breathing exercises. The system is contactless and operates in high-speed (25 measurements/second) with the measuring range of approximately 400×600×500mm in width, height and depth respectively. The accuracy of the calibrated apparatus is ±0.7mm.

The system can distinguish between different breathing patterns by means of determining the BPI (breathing pattern indicator). The accuracy of the measured volumes of chest wall deformation during breathing was verified with two standard methods of volume measurements. The results of the study show that the 3D measuring system with real-time respiration monitoring has great potential as a diagnostic and training assistance tool when monitoring the breathing pattern and evaluating the BPI, because it offers a simple on-screen graphical communication with the patient.

**Keywords:** three dimensional, real time, laser triangulation, breathing training, chest wall motion

## 1. Introduction

Measuring systems that monitor respiratory mechanics during breathing in real-time are becoming increasingly important in various fields of medicine. The measurements with standard methods and instruments such as plethysmographs [1], magnetometers [2, 3], stretching belts [4], and fiber optics [5] are mostly limited due to the invasiveness and its difficulty to use them in some measurement setups. Such devices also interfere with voluntary breathing and can consequently change the breathing pattern, therefore making volume measurements inaccurate.

Optical methods have an advantage over the standard methods of measurement because they do not disturb the breathing pattern due to the non-invasive principle. Current optical methods are mainly based on laser triangulation [6, 7], stereophotogrammetry [8, 9], photogrammetry [10], optoelectronic plethysmography [11, 12] and laser vibrometry [13]. The measurements are in some cases limited to measuring the displacements of only a certain number of predefined points (markers). The main drawback of markers is that their position needs to be determined prior to signal acquisition, which is often difficult and inconvenient.

One possible application of an optical measurement system is monitoring the respiratory mechanics during radiotherapy, where the patient needs a convenient real-time feedback in order to follow the instructions during the treatment [14]. Another application is a breathing training tool for patients with Chronic Obstructive Pulmonary Disease (COPD) [15]. In this case the system has to inform the patient about the active body regions in order to correct the breathing irregularities.

We present a 3D measuring system based on the laser multiple-line triangulation method. The system enables full-area real-time acquisition, processing and display with the frequency, which is limited by the frame rate of the camera (25Hz in our case). The accuracy of the system is validated by comparing the measured values to reference systems such as the spirometer and calibration syringe. Breathing pattern experiments are also performed in order to determine the system's potential training capabilities for the treatment of respiratory diseases.

\* klemen.povsic@fs.uni-lj.si; +386 1 4771-238; www.fs.uni-lj.si

## 2. Experimental setup

Figure 1 shows the two-sided measurement configuration, where the patient's chest wall and the back are acquired simultaneously by two independent measurement modules. The acquired 3D shape is displayed on a monitor for real-time breathing corrections during the breathing exercises.

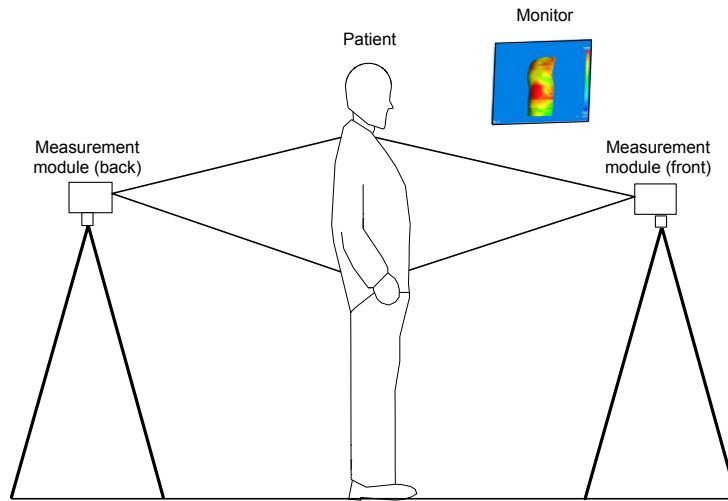


Fig. 1. Measurement setup.

Measuring modules are based on the multiple-line laser triangulation principle [16], which is shown in Figure 2. A laser diode projector (Lasiris SNF-533L) with 33 light planes was used in pair with a CCD (charge coupled device) camera (Sony XC-EI50CE) to obtain the shape information of the measured body. A narrow-band interference filter, which only allows the laser light to pass (centered at 670nm, 10nm FWHM), was placed between the lens and the camera's CCD sensor. This improves the contrast of the acquired image by reducing the effects of ambient light.

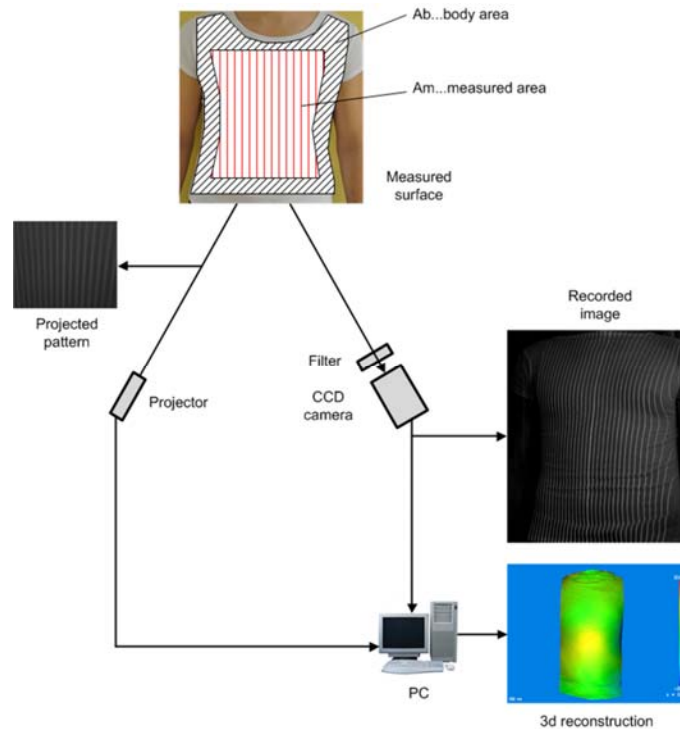


Fig. 2. Schematic diagram of the laser 3D measurement system.

The measuring modules were approximately 1.5m away from the patient. The measuring range depends on the camera's and projector's focal lengths, CCD sensor dimensions, the triangulation angle, and the distance between the laser projector and the camera. In our case, the range is approximately 400×600mm in width and height and approximately 500mm in depth with the accuracy of ±0.7mm. Dark skin or high ambient light have undesired effects on the laser lines detection, so in that case the patient should wear a white, thin elastic T-shirt, which reflects the light more effectively.

### 3. Real-time data processing

Figure 3 shows the real-time data processing diagram. In the initial step, the body area is manually determined by selecting the outline of the patient's torso and it remains constant for each measurement. After the acquisition, the line detection and line indexing are performed on the previously selected body area. The sub-pixel line-detection algorithm is based on the first derivative zero-crossing of the pixel values perpendicular to the lines. The measured area is calculated for each acquired image in such a way that it detects the outer laser lines and calculates the surface of the inner area, limited by these lines. With the system calibration, the transformation from two- to three- dimensional space finally occurs for every point of the detected line segment, after which the points in 3D space are analyzed and displayed in a shaded or color mode.

The entire process of 3D shape reconstruction is divided into four sequential transformations [17]: 1. transformation from the image coordinates to normalized distorted coordinates, 2. image distortion correction, 3. transformation to the 3D camera coordinate system and 4. transformation to the global coordinate system. The above steps are executed on all points of the detected line segments. Next, the points in 3D space are triangulated, displayed and analyzed to determine the breathing pattern and respiration waveform in real-time.

Surface displacements in the viewing direction of the camera are calculated by subtracting the current measured surface from the reference one. This is performed by using OpenGL architecture and a Z-buffer matrix, where the Z-coordinate of each point is saved [18]. Surface displacements are displayed with a color palette, where the blue color represents the inward (negative) and the red color represents the outward (positive) movement. With the calculation of the displacements on the reconstructed surface, the breathing pattern indicator (BPI) can be determined using the equation:

$$BPI = H_{ribcage} - H_{abdomen} \quad (1)$$

where  $H_{ribcage}$  and  $H_{abdomen}$  are the displacements of the selected points on the rib-cage and the abdomen respectively, in regards to the reference surface.

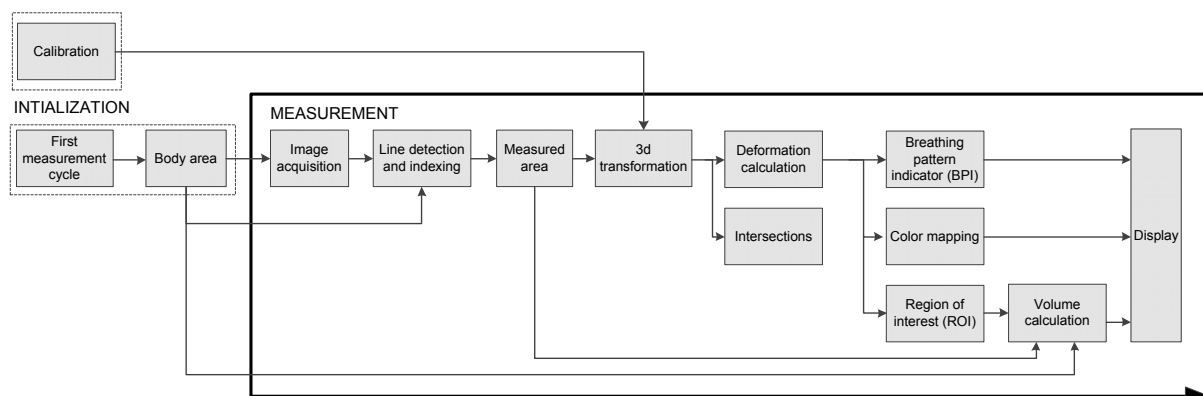


Fig. 3. Data processing diagram.

The surface deformation calculation over all points inside the Region of Interest (ROI) is based on mathematical integration and enables the observation of selected regions on the patient's torso. The ratio between the measured area ( $A_m$ ) and the body area ( $A_b$ ) is used for correcting the laser system's output

volumes (see Figure 2). We presumed that this correction would consider the areas on the patient's torso that move perpendicular to the viewing direction and are not visible to the measurement range of the apparatus. Consequently, the volume calculation for every acquired image is performed with the following equation:

$$V_c = V_M \cdot \frac{A_b}{A_m} \quad (2)$$

where  $V_M$  is the measured volume and  $V_c$  the volume corrected by the ratio between the body area  $A_b$  and the measured area  $A_m$ , both in pixels.

#### 4. Volume measurement tests

The accuracy of the laser 3D system was tested using standard methods of measuring volumes such as a calibration syringe and spirometer. For this purpose healthy adult male and female volunteers were measured.

The calibration syringe is a piston device for a steady and controlled injection of gas with the volume capacity of  $0.5\text{dm}^3$  and accuracy of 0.5%. Figure 4 shows the volume values acquired with the laser measuring system, when successively blowing  $0.5\text{dm}^3$  of air into the volunteer's mouth. The vertical step corresponds to the injection of air after which the values remain quite constant where the calibration syringe refill occurs. A nose-clip was used on the patient to cancel out the loss of injected air through the nasal airway.

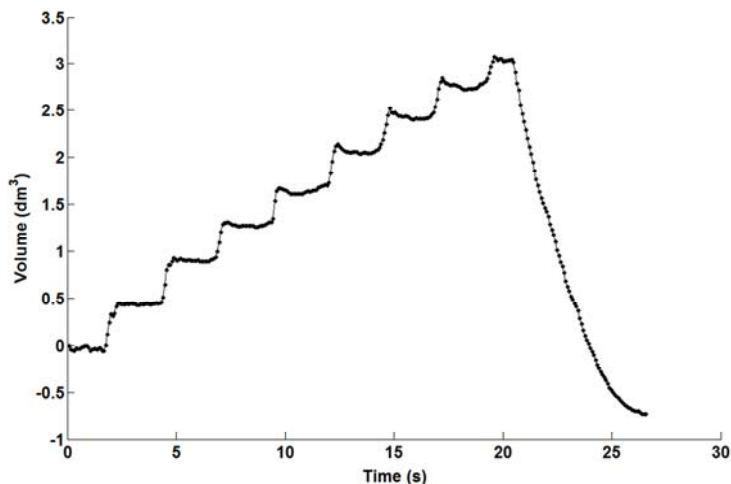


Fig. 4. The chest volume difference measurement during successively blowing  $0.5\text{dm}^3$  air into the lungs.

The second verification was performed using a spirometer (Jaeger MasterScope Rhino), which is an apparatus for measuring the volume of air inspired and expired by the lungs during ventilation. It measures the flow from 0.2 to 12 L/s with an accuracy of  $\pm 2\%$ . Verification with a spirometer is based on normal breathing cycles where the amplitude between inhalation and exhalation is used as a reference. The amplitude between successive breathing cycles was calculated based on peak and valley detection. Figure 5 shows the respiration waveforms measured by a laser and a spirometer simultaneously. Throughout the duration of the entire breathing cycle of approximately 40 seconds, it is clearly visible that the volumes measured by the laser sufficiently follow the spirometer's volumes.

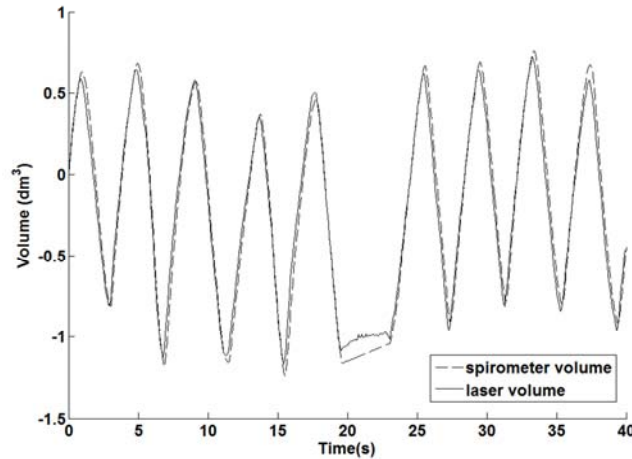


Fig. 5. Respiration waveforms measured with laser (—) and spirometer (---).

After the tests, the values of the laser measuring system and the calibration syringe were linearly interpolated. Although the correlation between the measured volumes is high ( $R = 0.998$ ), the slopes of the lines for individual measurements show poor repeatability by varying more than 10%. Similarly, the volumes verified with the spirometer were also analyzed. In this case, the results are better as they are more repeatable (error less than 5%) in comparison to the calibration syringe tests.

We estimate that the main reason the calibration syringe tests achieve less accurate and less repeatable results is in the physiological characteristics of the human respiratory mechanics. When the air is forcibly injected into the lungs it remains in the windpipe or mouth. As this is invisible to our laser measuring system, these effects greatly contribute to the inaccuracy of the measurements. During the insufflation of the air, the breathing diaphragm moves toward the abdominal cavity, which results in a smaller displacement of the thoraco-abdominal wall than that expected from the insufflated volume. Furthermore, when the lungs expand above the limit of shallow respiration, the expansion of the lungs occur in all directions, which are not in the range of the laser's measurement area.

The breathing was more steady and shallow and therefore the lungs expansion was mainly frontal when the spirometer was used. The volume measured by the laser system is evidently more accurate in this case, as it covers the entire frontal area of the volunteer.

## 5. Breathing training assistance

The surface displacements and depth by color representation is one of the main advantages of this 3D measuring system (see Figure 6 and Figure 7). It enables simple and effective visualization of the thoraco-abdominal displacements in real-time, which is potentially useful for breathing assistance during therapy.

Figure 6 represents a series of 3D shape measurements for a single subject with the rib-cage-dominant breathing pattern. The upper row shows the chest wall displacement (front) and the bottom row the displacement of the back. As the red and blue colors expose the most active regions, it can be noticed that the upper chest part moves outward from the body, and that the bottom part stays in the same position or even goes a little inward. With inhalation of air into the lungs, the lower end of the back moves slightly inward, where the other areas on the back remain in somewhat constant position. The looseness of the shirt that the patient was wearing in order to reflect the projected light efficiently is partially responsible for the results described above.

The abdomen-dominant breathing for a male subject is shown in Figure 7. It is clearly visible that the entire abdomen moves uniformly outward. The displacements on the back of the torso are small and more or less uniform throughout the entire measurement.

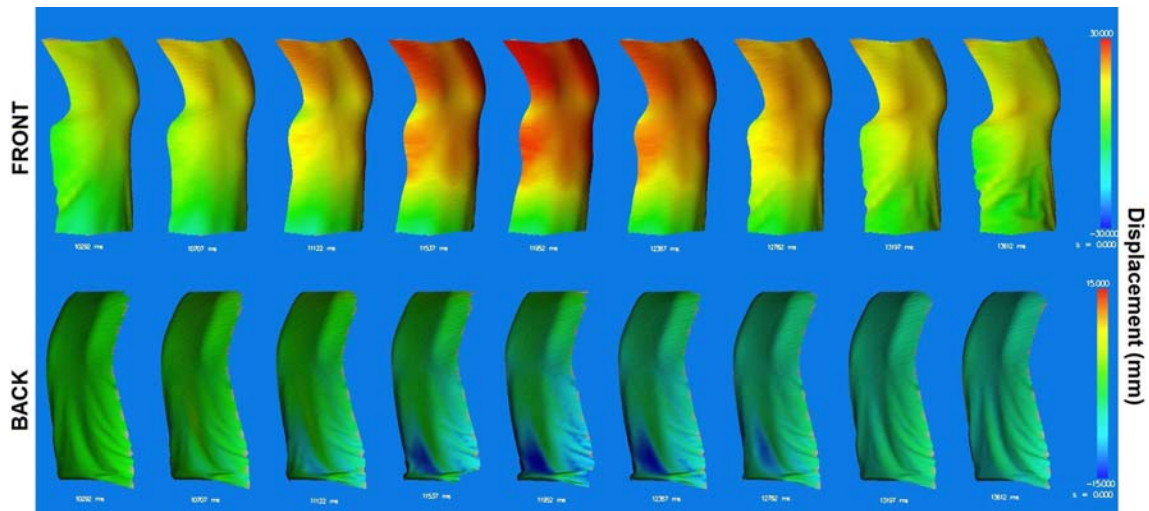


Fig. 6. 3D measurements of the front and the back of the torso for the rib-cage-dominant breathing (male subject).

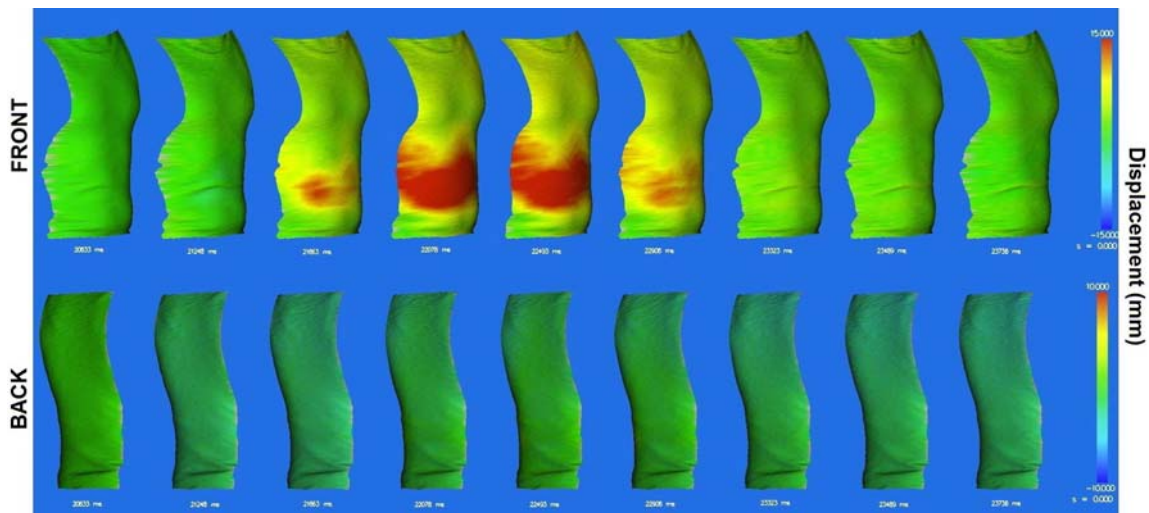


Fig. 7. 3D measurements of the front and the back of the torso for the abdomen-dominant breathing (male subject).

By calculating the breathing pattern indicator (BPI) in addition to color representation, the breathing pattern can be determined even more accurately. The difference between the BPI of the abdomen-dominant and the rib-cage-dominant breathing for each individual subject is clearly visible from Figure 8, where the differences between the rib-cage and abdomen area are shown. The abdomen-dominant breathing is mainly performed with the abdominal region, where the slight movements of the rib-cage follow the outward motion of the abdomen. This accounts for the relatively small displacement difference. On the contrary, the rib-cage-dominant breathing shows that the displacements between both regions are greater due to the simultaneous outward movement of the rib-cage and the inward movement of the abdomen. Connecting the maximum BPI values of each breathing cycle, the curve for the distinct breathing pattern can be constructed (see Figure 8). Next, the BPI threshold can be defined, above which the breathing can be considered mostly as rib-cage-dominant. In turn, the BPI values below the threshold suggest abdomen-dominant breathing pattern.

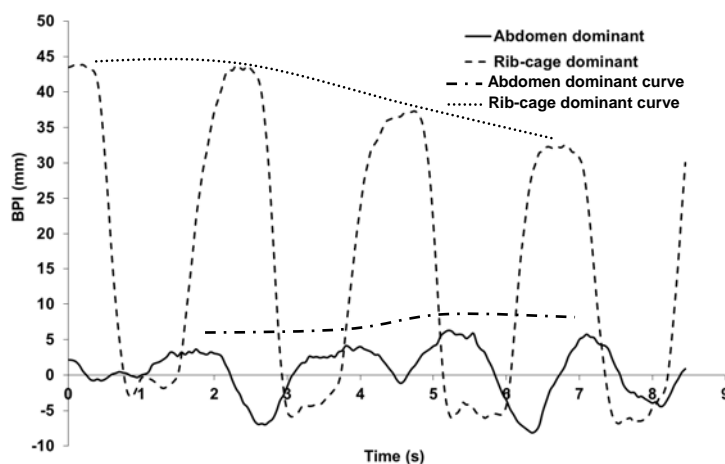


Fig. 8. BPI (breathing pattern indicator) of rib cage and abdomen in case of the abdomen-dominant (—) and the rib-cage-dominant (---) type of breathing with respective curves connecting the maximum values of breathing pattern indicator (BPI).

## 6. Conclusion

A 3D measuring system for breathing training and assistance in real-time based on the multiple-line triangulation principle is presented. Its advantage is in contactless, full-area measurement operating at high-speed (25 measurements/second), while maintaining full portability. The color representation of active body regions is easy to understand and the breathing pattern indicator (BPI) offers additional help in determining the breathing pattern more accurately. The shape of the surface is measured with the accuracy of  $\pm 0.7$ mm, with the measuring range of approximately 400 x 600 x 500 mm in width, height and depth, respectively.

The results of the study clearly show that the 3d measuring system has a lot of potential and possibilities when monitoring and training breathing, because it offers a simple, intuitive and effective method of communication with the patient. The system does not interfere with the human respiratory mechanics, therefore providing more accurate results and simultaneously physically relieving the patient.

## Acknowledgments

This work was supported by the Slovenian Research Agency under the applied research project (L7-9391).

## References

- [1] Black, A. M. S., Bambridge, A., Kunst, G., and Millard, R. K., (2001): "Progress in non-invasive respiratory monitoring using uncalibrated breathing movement components", *Physiological Measurement*, Vol.22, No.1, pp.245-261.
- [2] Gilbert, R., Auchincloss, J. H. Jr., Brodsky, J., and Boden, W., (1972): "Changes in tidal volume, frequency, and ventilation induced by their measurement", *J. Appl. Physiol.*, Vol.33, No.2, pp.252-254.
- [3] Loring, S. H., Townsend, S. R., Gallagher, D. C., Matus, H. L., Tegins, E. O., Kopman, D. F., and Schwartzstein, R. M., (2006): "Expiratory Abdominal Rounding in Acute Dyspnea Suggests Congestive Heart Failure", *Lung*, Vol.184, No.6, pp.324-329.
- [4] Binks, A. P., Banzett, R. B., and Duvivier, C., (2007): "An inexpensive, MRI compatible device to measure tidal volume from chest-wall circumference", *Physiological Measurement*, Vol.28, No.2, pp.149-159.
- [5] Augousti, A. T., Maletras, F. X., and Mason, J., (2005): "Improved fibre optic respiratory monitoring using a figure-of-eight coil", *Physiological Measurement*, Vol.26, No.5, pp.585-590.

- [6] T. Kondo, S. Minocchieri, D. N. Baldwin, M. Nelle, and U. Frey, "Noninvasive monitoring of chest wall movement in infants using laser," *Pediatric Pulmonology* 41(10), 985-992 (2006).
- [7] Drummond, G. B., and Duffy, N. D., "A video-based optical system for rapid measurements of chest wall movement", *Physiological Measurement*, Vol.22, No.3, pp.489-503.
- [8] Cala, S. J., Kenyon, C. M., Ferrigno, G., Carnevali, P., Aliverti, A., Pedotti, A., Macklem, P. T., and Rochester, D. F., (1996): "Chest wall and lung volume estimation by optical reflectance motion analysis", *Journal of Applied Physiology*, Vol. 81, No.6, pp.2680-2689.
- [9] Grotte, A.D., Wantier, M., Cheron, G., Estenne, M., and Paiva, M., (1997): "Chest wall motion during tidal breathing", *J. Appl. Physiol.*, Vol.83, No.5, pp.1531-1537.
- [10] Ricieri, D. D. and Rosario, N. A., "Effectiveness of a photogrammetric model for the analysis of thoracoabdominal respiratory mechanics in the assessment of isovolume maneuvers in children", *Jornal Brasileiro De Pneumologia*, Vol.35, No.2, pp.144-150.
- [11] Dellaca, R. L., Ventura, M. L., Zannin, E., Natile, M., Pedotti, A., and Tagliabue, P., (2010): "Measurement of Total and Compartmental Lung Volume Changes in Newborns by Optoelectronic Plethysmography", *Pediatric Research*, Vol.67, No.1, pp.11-16.
- [12] Aliverti, A., Carlesso, E., Dellaca, R., Pelosi, P., Chiumello, D., Pedotti, A., and Gattinoni, L., (2006): "Chest wall mechanics during pressure support ventilation", *Critical Care*, Vol.10, No.2, pp.1-10.
- [13] Scalise, L., Marchionni, P., and Ercoli, I., (2010): "A non-contact optical procedure for precise measurement of respiration rate and flow", *Biophotonics: Photonic Solutions for Better Health Care II*, USA.
- [14] Nakamura, K., Shioyama, Y., Nomoto, S., Ohga, S., Toba, T., Yoshitake, T., Anai, S., Terashima, H., and Honda, H., (2007): "Reproducibility of the abdominal and chest wall position by voluntary breath-hold technique using a laser-based monitoring and visual feedback system", *International Journal of Radiation Oncology, Biology, Physics*, Vol.68, No.1, pp.267-272.
- [15] Alves, G. S., Brito, R. R., Campos, F. C., Vilaca, A. B. O., Moraes, K. S., and Parreira, V. F., (2008): "Breathing pattern and thoracoabdominal motion during exercise in chronic obstructive pulmonary disease", *Brazilian Journal of Medical and Biological Research*, Vol.41, No.11, pp.945-950.
- [16] Jezeršek, M., Povšič, K., Fležar, M., Topole, E., and Možina, J., (2010): "Laser based method for real-time three-dimensional monitoring of chest wall movement", *Real-Time Image and Video Processing 2010*, Belgium.
- [17] Jezeršek, M., and Možina, J., (2009): "High-speed measurement of foot shape based on multiple-laser-plane triangulation", *Opt. eng.*, Vol.48, No.11, pp.113604-1-113604-8.
- [18] Shreiner, D., (2010): "The OpenGL Programming Guide: The Official Guide to Learning OpenGL Version 3.0 and 3.1", 7th Edition, Addison-Wesley Professional, NJ.